

# Reinforcement of Calcium Phosphate Cement with E-Glass Fibre

Sudip Dasgupta, Debosmita Pani, Kanchan Maji

**Abstract**—Calcium Phosphate Cement (CPC) due to its high bioactivity and optimum bioresorbability shows excellent bone regeneration capability. Despite it has limited applications as bone implant due to its macro-porous microstructure causing its poor mechanical strength. The reinforcement of apatitic CPCs with biocompatible fibre glass phase is an attractive area of research to improve upon its mechanical strength. Here, we study the setting behaviour of Si-doped and un-doped  $\alpha$  tri calcium phosphate ( $\alpha$ -TCP) based CPC and its reinforcement with addition of E-glass fibre. Alpha Tri calcium phosphate powders were prepared by solid state sintering of  $\text{CaCO}_3$ ,  $\text{CaHPO}_4$  and Tetra Ethyl Ortho Silicate (TEOS) was used as silicon source to synthesize Si doped  $\alpha$ -TCP powders. Both initial and final setting time of the developed cement was delayed because of Si addition. Crystalline phases of HA (JCPDS 9-432),  $\alpha$ -TCP (JCPDS 29-359) and  $\beta$ -TCP (JCPDS 9-169) were detected in the X-ray diffraction (XRD) pattern after immersion of CPC in simulated body fluid (SBF) for 0 hours to 10 days. As Si incorporation in the crystal lattice stabilized the TCP phase, Si doped CPC showed little slower rate of conversion into HA phase as compared to un-doped CPC. The SEM image of the microstructure of hardened CPC showed lower grain size of HA in un-doped CPC because of premature setting and faster hydrolysis of un-doped CPC in SBF as compared that in Si-doped CPC. Premature setting caused generation of micro and macro porosity in un-doped CPC structure which resulted in its lower mechanical strength as compared to that in Si-doped CPC. It was found that addition of 10 wt% of E-glass fibre into Si-doped  $\alpha$ -TCP increased the average DTS of CPC from 8 MPa to 15 MPa as the fibres could resist the propagation of crack by deflecting the crack tip. Our study shows that biocompatible E-glass fibre in optimum proportion in CPC matrix can enhance the mechanical strength of CPC without affecting its biocompatibility.

**Keywords**—Calcium phosphate cement, biocompatibility, e-glass fibre, diametral tensile strength.

## I. INTRODUCTION

CALCIUM Phosphate Cements (CPC) by virtue of its excellent biocompatibility, osteoconductivity and bioresorbability are established materials for the augmentation of bone defects [1], [2]. One of the main advantages of CPC is its in vivo hardening ability under physiological environment. A hardened and set CPC matrix comprises a network of entangled calcium phosphate crystals whose chemical composition and crystal size that can be tailored to closely resemble the biological hydroxyapatite present in living bone [3], [4].

D. Pani and K. Maji are with the Ceramic Engineering Department, National Institute of Technology, Rourkela, 769008, India (e-mail: pani.debasmita317@gmail.com, kanchan.maji@gmail.com).

S. Dasgupta is with the Ceramic Engineering Department, National Institute of Technology, Rourkela, 769008, India (Corresponding author, e-mail: dasguptas@nitrkl.ac.in).

CPC mouldable pastes can be used as filler to reconstruct bone defects. In certain cases, it can be injected in the surgical site using minimally invasive surgical procedures [5], [6], that can treat several clinical situations such as osteoporosis related fractures, unstable fractures, maxillofacial defects and deformities, and more recently can be applied for vertebroplasty [7]. However, not only in terms of strength, but especially in terms of toughness, ductility, and fatigue resistance its properties are far from those of the cortical or even the cancellous bone. This poor mechanical performance has limited its applicability to non-stress-bearing sites. Nonetheless, the major limitation to mechanical performance of CPC stems from its intrinsic brittleness and porosity that vary between 20% and 50% depending on the liquid to powder ratio used in its preparation [8]. Thus, the bending strength of CPC, typically in the range of 5–15 MPa [9] falls well below that of cortical bone (200 MPa) [10]. Again the reported value of fracture toughness of CPC [11] of 0, 14 MPa  $\text{m}^{1/2}$  is far from the fracture toughness of human cortical bone, 2–5 MPa  $\text{m}^{1/2}$  [12]. CPC with enhanced toughness has the potential to repair major bone defects, such as the repair of multiple fractures of long bones, fixing of cemented articulation prostheses. Keeping in view of bioresorbability and bone regeneration capability of CPC particularly it is important to have CPC with enhanced mechanical properties at the initial stages after implantation. This has led to the development of fibre-reinforced CPC.

Reinforcement of brittle CPC with fibres [13] particularly toughening by long continuous fibres [14] is one of the most successful approaches in enhancing its mechanical behavior. Reinforcement with resorbable fibre [15]-[18] requires precise control over its biodegradability to eliminate the danger of strength degradation of CPC during the course bone healing. On the contrary, addition of non-resorbable fibres in resorbable cement matrices would result in fibre release in the surrounding tissues, with the subsequent biocompatibility risks. In this sense, fibre dimension, biocompatibility, and osteoconductivity of fibre material are critical issues. For biocompatible and big fibre sizes possibly the risk is only the formation of fibrous tissue around the fibres. The most critical case would be for reinforcement of CPC with carbon nanotubes [19], because of its nanometric size and tendency towards bioaccumulation eliciting unwanted foreign body response. Other reinforcing synthetic fibres such as polyamide [20], aramide [21] may suffer from lack of biocompatibility in CPC matrix under physiological conditions. E-glass fibres are composed of an alumino-borosilicate glass with less than 1 wt% alkali oxides, mainly biocompatible and bioinert

material, can serve as one of the best alternatives among non resorbable fibres as reinforcing agent to CPC matrix. In this case, we investigated the reinforcing effect of E-glass fibre addition into Si-doped  $\alpha$  tri calcium phosphate ( $\alpha$ -TCP) based CPC and its influence on overall biocompatibility and osteoconductivity of CPC. To improve adhesion between the fibres and the CPC matrix to further enhance mechanical properties, E-glass fibres were coated with apatite using a biomimetic process. Setting time, phase composition, hydrolysis conversion rate, microstructure, and diametral tensile strength (DTS) of E-glass fibre reinforced undoped and Si-doped CPC were studied and compared. Biocompatibility of fibre reinforced CPC was assessed using MTT assay after culturing mesenchymal stem cell (MSC) on setCPC.

## II. MATERIALS

Calcium carbonate  $\text{CaCO}_3$  [Vico Trading and Production Co. Ltd (Vietnam)], Calcium hydrogen phosphate (Sigma, India), Tri-ethyl ortho silicate (TEOS) (Powertrain Engineering Trappes, France), Di-sodium hydrogen phosphate ( $\text{Na}_2\text{HPO}_4$ ) (Shanghai Orgpharma Chemical Co. Ltd, China), E-glass fibre (Binani Pvt Ltd, INDIA), hydrochloric acid (37 vol%) and Tris buffer  $[(\text{CH}_2\text{OH})_3\text{CNH}_2]$  [Angus Chemical Company (Buffalo Grove, US)] were purchased and used without further purification.

## III. METHODS

### A. Synthesis of Doped and Pure $\alpha$ Tricalcium Phosphate

At first hydrated di-calcium phosphate (DCPD) was heated at  $180^\circ\text{C}$  for 4 hours to convert it to DCPA. DCPA and  $\text{CaCO}_3$  were taken in the molar ratio of 2:1 were then ball milled in iso-1-propanol for 12 hours for uniform mixing followed by drying in oven at  $100^\circ\text{C}$ . Next the dried sample was then crushed to powder and was sintered at  $1300^\circ\text{C}$  for a period of 4 hours followed by rapid air quenching of the samples. After sintering the sample was ground and sieved through 100 mesh. To synthesize 1 mol % Si doped TCP, nearly 0.13 ml TEOS was added to the mixture of DCPA and  $\text{CaCO}_3$  and then ball milled in isopropanol followed by drying, sintering, grinding and sieving of the synthesized powders.

### B. Preparation of Anhydrous Sodium Hydrogen Phosphate Solution

Required amount of  $\text{HNa}_2\text{O}_4\text{P}$  (formula mass= 141.98 and density= 1.7gm/cc) was dispersed in distilled water to prepare 5 vol% solutions of sodium hydrogen phosphate.

### C. Preparation of SBF Solution

Simulated Body Fluid was prepared by the standard Kokubo's method [22]. In brief, the chemicals listed in Table I was dissolved in distilled water following the same sequence and then pH of the solution was adjusted to 7.4 using tris buffer and HCl.

### D. Preparation of Hydroxyapatite Coated E-Glass Fibre

E-glass fibres were cut into approximately 1 mm length and immersed in SBF solution for about 14 days. The SBF

solution was renewed after every 3 days upto 14 days of immersion time. After 14 days, E-glass fibres were filtered out, washed with deionised water to remove any unwanted salt adhered to its surface and then freeze dried.

TABLE I  
CHEMICAL COMPOSITION OF SBF SOLUTIONS

Order	Reagent	Amount (gpl)
1	NaCl	6.547
2	NaHCO <sub>3</sub>	2.268
3	KCl	0.373
4	Na <sub>2</sub> HPO <sub>4</sub> .2H <sub>2</sub> O	0.178
5	MgCl <sub>2</sub> .6H <sub>2</sub> O	0.305
6	CaCl <sub>2</sub> .2H <sub>2</sub> O	0.368
7	Na <sub>2</sub> SO <sub>4</sub>	0.071
8	(CH <sub>2</sub> OH) <sub>3</sub> CNH <sub>2</sub>	6.057
9	HCl	40mL

### E. Preparation of Sample for Studying Setting and Hardening

Pure and Si doped TCP powder and  $\text{Na}_2\text{HPO}_4$  solution were mixed in a weight ratio of 3:1 to form a viscous and mouldable paste that was filled into a cylindrical silicon mould with a diameter of 10 mm and a height of 15 mm. The samples in the mold were maintained for 1 hour at 100% relative humidity (R. H.) and room temperature of  $26 \pm 1^\circ\text{C}$ . Cylinders of cement were removed from the mould and immersed in SBF at  $37^\circ\text{C}$  for 1 to 10 days. A batch of Si doped  $\alpha$ -TCP powder and 10 wt% E-glass fibres was prepared by proper and uniform mixing and used for making set and hardened CPC cylinders according to the procedure mentioned above. For each period, 5 samples were prepared.

## IV. CHARACTERIZATION

### A. XRD Analysis

X-ray diffraction analysis of the  $\alpha$ -Tricalcium phosphate and Si doped  $\alpha$ -tricalcium phosphate powders and set CPC were performed using  $\text{CuK}_\alpha$  radiation ( $1.54 \text{ \AA}$ ) on a diffractometer (Rigaku Ultima IV, Japan) fitted with Ni filter and operated at 40KV and 40 mA. Data were collected by using solid state detector with scanning range of  $2\theta=10^\circ-70^\circ$ , and a  $2\theta$  step size of  $5^\circ/\text{min}$ . XRD analysis of the powder samples was performed using X'PERT HIGH SCORE software.

### B. Hardening and Setting

The undoped and doped TCP powders and powders mixed with 10 wt% E-glass fibres were processed for setting of CPC according to the methods discussed in Section III and V. Initial (I) and final (F) setting times were measured using the Gillmore needles (ASTM, 2000) following the standard protocol. All measurements were performed at room temperature. The setting times were obtained from a set of three samples of doped and undoped  $\alpha$ -tricalcium phosphate based CPC in each category.

### C. Study of Kinetics of Setting Reaction in CPC

Samples of set cement were removed from the mould and immersed in SBF at 37 °C for 10 days. At intervals of 0 hour, 10 hour, 1 day, 2 days and upto 10 days the immersed samples were removed from the SBF solution. The samples were then crushed to powder and immersed into acetone to stop the hydraulic setting reaction at that specific time point. Putting the samples onto acetone arrests the  $\alpha$ -TCP to HA conversion reaction at that point. After drying in air the powdered samples were recorded for x-ray diffraction pattern. In x-ray diffraction pattern, the intensities of  $\alpha$ -TCP peak having d spacing of 2.905 Å at crystal plane of (170) and hydroxyapatite's (211) crystal plane having d spacing of 2.814 were chosen to calculate the relative amount of respective phases present in the sample. The extent of conversion of  $\alpha$ -TCP into HA was calculated using (1):

$$\text{Conversion (weightfraction)} = \frac{[(I_o / I_s) - (I_t / I_s)]}{[(I_o / I_s) - (I_\infty / I_s)]} \quad (1)$$

where,  $I_o$  = integrated intensity of the peaks corresponding to the converted phase at the beginning,  $I_t$  = integrated intensity of the peaks corresponding to the converted phase at time t,  $I_\infty$  = integrated intensity of the peaks corresponding to the converted phase at infinite time,  $I_s$  = integrated intensity of the peak corresponding to the internal standard.

### D. Determination of Mechanical Strength

The set CPC samples were removed from the mould and immersed in SBF solution at 37.5°C. Samples were taken out from SBF solution at periodic time intervals for use as test specimens to measure diametral tensile strength (DTS) using Universal Testing Machine (Tinius Olsen H10KS). Load was applied at a speed of 1mm/min at room temperature until failure. Three replicas of each kind of CPC samples were tested for measuring DTS.

DTS of the specimens was calculated using (2):

$$\text{DTS} = 2\sigma / \pi \cdot d \cdot t \quad (2)$$

where,  $\sigma$  = Load in Kg force,  $\pi$  = constant (3.14), d = diameter of the samples (mm), t = thickness of the samples (mm)

### E. Analysis of Microstructure Using Scanning Electron Microscopy

CPC samples were taken out from SBF after definite time interval and dried in air. To examine the microstructure of set CPC sample, it was graphite coated by sputtering and then analysed using scanning electron microscopy (NOVA NANO SEM FEG) operated at 310V and 90µA. Microstructure and elemental composition of uncoated and SBF treated E-glass fibre were observed using the same method and with an EDX detector fitted to scanning electron microscope.

### F. Study on Cytotoxicity of CPC Using MTT Assay

Viability of mesenchymal stem cells (MSC) cultured onto the CPC samples were determined after performing [3-(4,5-dimethylthiazol-2-yl)-2,5-diphenyltetrazolium bromide]

(MTT) assay. We note that for the MTT assay, the amount of produced formazan crystal is proportional to the number of viable cells present in the CPC sample. In brief, Si doped CPC and fibre reinforced CPC samples were submerged in DMEM cell culture media and MSCs were seeded to each sample at  $1 \times 10^6$  cells per well and incubated for 3, 7, and 11 days with replacement of DMEM after every 2 days of culture. After each day interval of culture point, 20 µL (0.5 mg/mL) MTT solution was added onto each sample placed in 24 well plate. The samples containing MSCs and MTT solution were then incubated for another 3.5 h at 37° C. The precipitated purple coloured formazan crystals were dissolved in 150 µL of MTT solvent by shaking the plate for 15 min. Then the solutions were taken out in ependrofs, centrifuged and the supernatant was transferred into another 96- well plate to record the absorbance at 595 nm using a micro-plate reader (Bio-Tek ELx800).

## V. RESULTS AND DISCUSSION

### A. Phase Evaluation of Synthesized $\alpha$ -TCP Powders

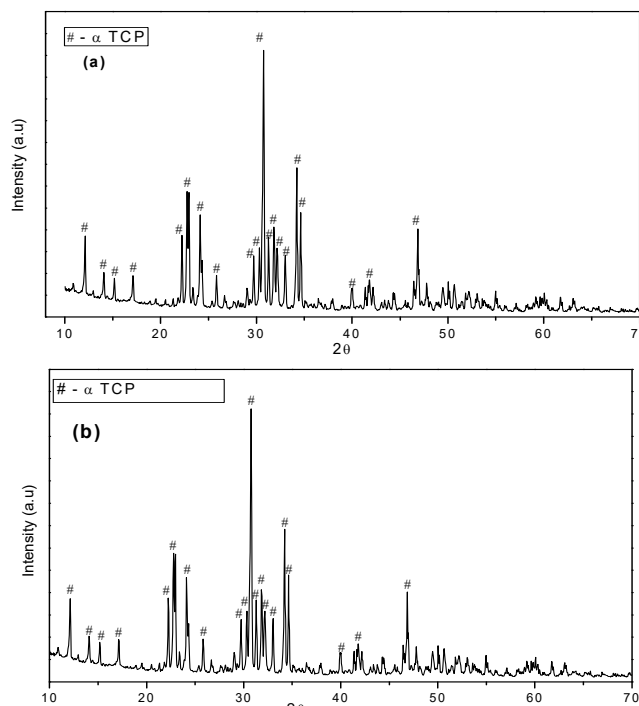


Fig. 1 X-ray diffraction pattern of as synthesized  $\alpha$  TCP powders (a) undoped (b) Si doped

Fig. 1 shows the x-ray diffraction pattern of  $\alpha$ -TCP powder synthesized using solid state reaction between calcium carbonate and anhydrous di-calcium phosphate at 1300°C for 6 hours. The x-ray diffraction patterns of undoped  $\alpha$ -TCP and 1 mol% Si doped  $\alpha$ -TCP powders revealed the presence of  $\alpha$ -TCP as major phase with traces of  $\beta$ -TCP in it. Rapid quenching of hot reaction product from 1300°C to room temperature allowed the metastable  $\alpha$ -TCP to appear as major phase in the synthesized powder.

**B. Setting of CPC Samples**

Both initial and final setting time of CPC samples are shown in Table II. It is evident that 1 mol% Si doping delayed the setting behaviour of the CPC.  $\alpha$ -TCP hydrolyzes into HA to grow

TABLE II  
 SETTING TIME OF CPC SAMPLES

Sample	Initial setting time (min)	Final setting time (min)
Un-doped CPC	12	38
Si doped CPC	18	55

HA crystals in an entangled manner to give strength to the structure and when compressive strength of CPC reaches to 1 MPa, initial setting time is recorded. Si doping stabilizes the  $\alpha$ -TCP phase and retards HA crystal growth, thus delayed the setting behaviour of  $\alpha$ -TCP based cement.

**C. Kinetics of Conversion into HA**

Figs. 2 and 3 demonstrate the XRD patterns of the calcium phosphate cement derived from hydrolysis of  $\alpha$ -TCP crystals in SBF solutions at different periods up to 10 days. The intensities of the  $\alpha$ -TCP peaks at 22.2° (201) and 24.1° (161,-331) decreased when the time of immersion in SBF increased from 0 day to 10 days, due to its transformation into HA. From the XRD pattern it is evident that increasing amount of HA phase was evolved in CPC due to hydrolysis of  $\alpha$ -TCP into HA with increase in immersion time in SBF.

Si doped CPC showed little slower rate of conversion into HA phase as compared to un-doped CPC. Si doped  $\alpha$ -TCP cements presented a faster initial reaction than pure  $\alpha$ -TCP but a slower secondary reaction.

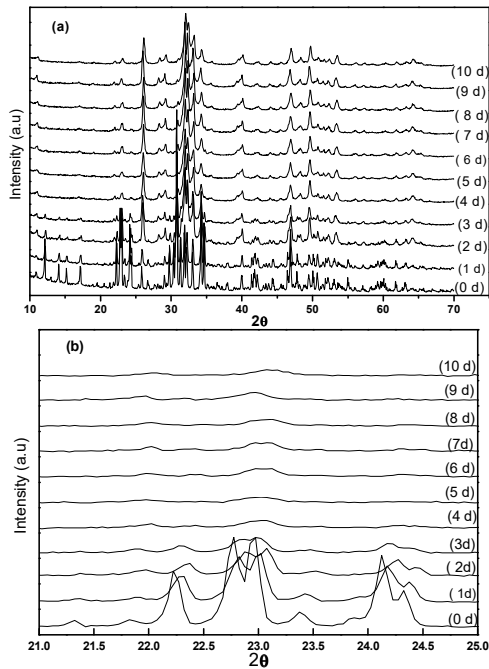


Fig. 2 XRD pattern of undoped CPC in SBF with 2θ varying from (a) 10-70° (b) 20- 25°

TABLE III  
 FITTING OF  $\alpha$  TCP TO HA CONVERSION EQUATION

Equation	Undoped CPC (a)	Si doped CPC (b)
$[X= X_o- A \exp(-kt)]$	$X= 1.0513-1.1219\exp(-0.01253t)$	$X= 1.0567-1.1219\exp(-0.01t)$
R <sup>2</sup>	0.99584	0.989
k (Rate Constant) (hour <sup>-1</sup> )	0.01253	0.010

The plot of conversion degree vs. immersion time in SBF for doped and undoped CPC is displayed in Fig. 4. The experimental points fitted very well with (3) proposed by [23] for conventional  $\alpha$ -TCP cement.

$$\text{Conv} ( X ) = X_o - A \exp ( -kt ) \quad (3)$$

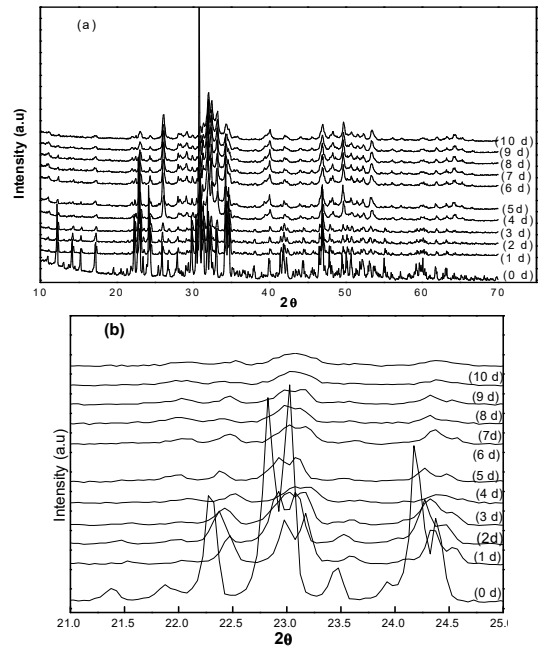


Fig. 3 XRD pattern of Si doped CPC in SBF with 2θ varying from (a) 10-70° (b) 20- 25°

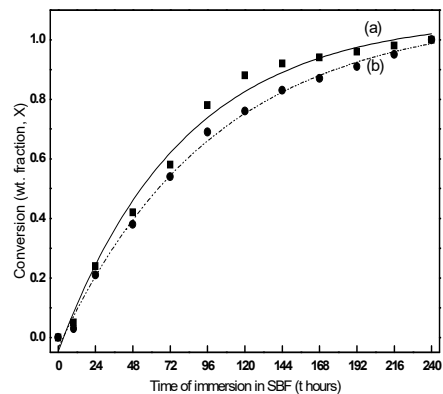


Fig. 4 Comparison of conversion rate of (a) undoped and (b) Si doped CPC

Data fitted very well with the Exponential Equation and the correlation coefficients obtained were 0.9958 and 0.989 for un-doped and Si doped CPC, respectively. The calculated rate

constant for hydrolysis of  $\alpha$ -TCP,  $k$  value of (1), for un-doped CPC was found to be  $0.01253 \text{ hour}^{-1}$ , whereas that for Si doped CPC came out to be  $0.01 \text{ hour}^{-1}$  (Table III). It is evident from Fig. 4 that throughout the period of immersion in SBF, Si-doped  $\alpha$ -TCP based cement showed a slower rate of conversion into hydroxyapatite as compared to un-doped  $\alpha$ -TCP based calcium phosphate cement because Silicon stabilized the  $\alpha$ -TCP phase and thus retarded its hydrolysis into HA in SBF.

#### D. Microstructural Observation of Set Cements Using SEM

Scanning Electron Microscopy examination of the fully set cements soaked in SBF for 10 days at  $37^\circ\text{C}$  showed the formation of a thin and dense bonelike apatite layer on their surface, Fig. 5 (a). The newly formed apatite layer consisted of nodules of crystal platelets grown together, forming a compact layer. The examination with SEM of the set cement showed a network of entangled plate-like apatite crystals grown from the  $\alpha$ -TCP grains. Typical Hadley grains could be observed showing an empty thick shell of hydration products inside which an  $\alpha$ -TCP grain had fully reacted.

Fig. 5 (b) shows the growth of spherical HA crystals in Si doped CPC. Here the hydroxyapatite crystals were larger in

size and more spherical in morphology as compared to un-doped CPC. The hardened CPC showed lower grain size of HA in un-doped CPC because of premature setting and faster hydrolysis of un-doped  $\alpha$ -TCP in SBF as compared that in Si-doped CPC. Premature setting caused generation of micro and macro porosity in un-doped CPC structure, whereas Si doped CPC represented a microstructure with lower porosity and greater compactness because of more delayed and controlled growth of HA crystals.

#### E. Composition of E- Glass Fibre

Fig. 6 (a) shows image of E-Glass fibres obtained using scanning electron microscopy. E-glass fibres having an average diameter of  $14 \mu\text{m}$  and length of 1.2-1.6 mm were used for reinforcing CPC matrix. EDAX analysis of the procured E-Glass fibre is shown in Fig. 6 (b) and the elemental composition is given in Table IV. E-glass fibres are primarily aluminoborosilicate glass, but detection of B is beyond the reach of the EDAX detector. The presence of  $\text{Al}_2\text{O}_3$  in the silica glass fibre gives necessary strength and chemical resistance to glass fibre so that it can be used for reinforcement of CPC matrix.

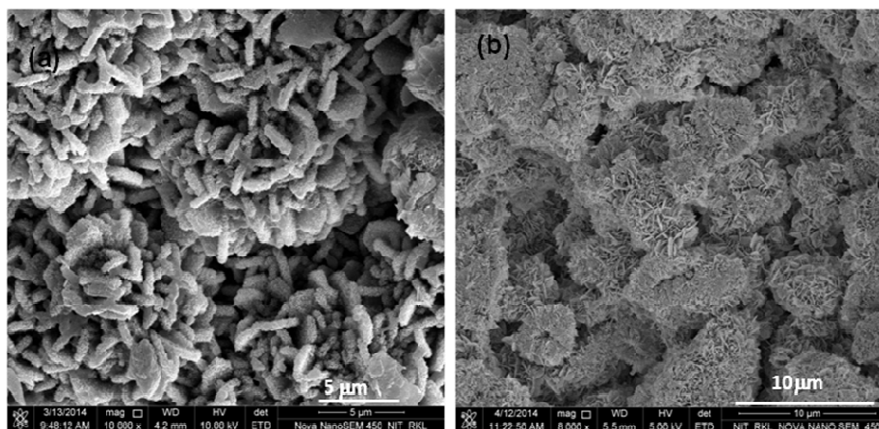


Fig. 5 SEM micrographs of set cement after 10 days in SBF (a) un-doped CPC (b) Si doped CPC

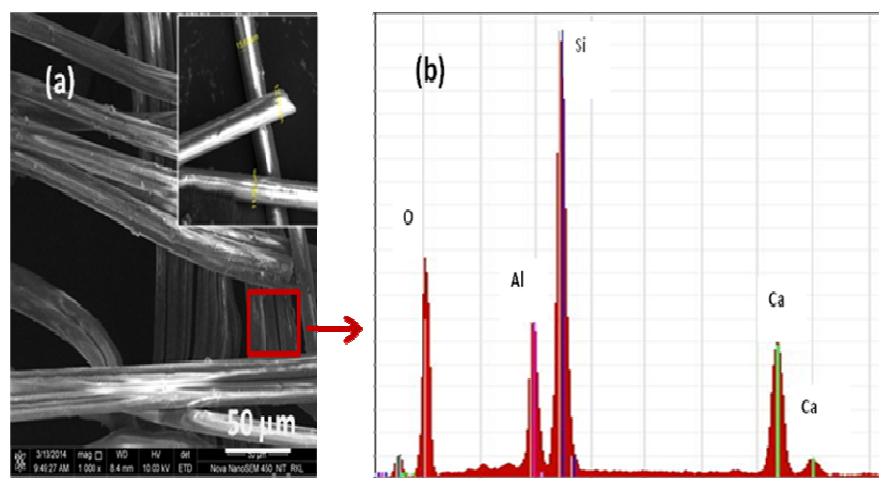


Fig. 6 (a) FESEM micrograph of E-glass fibre (b) EDAX analysis of E-glass fibre

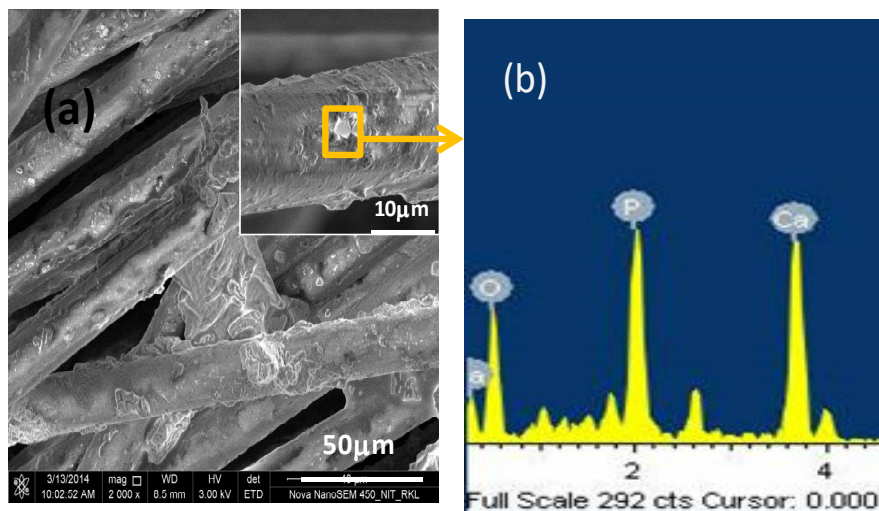


Fig. 7 (a) FESEM micrograph of SBF treated E- glass fibre (b) EDAX analysis of coated surface of E-glass fibre

TABLE IV  
QUANTITATIVE ANALYSIS OF E- GLASS FIBRE FROM EDAX DATA

Element	Atomic No	Weight %
O	8	50.26
Ca	20	16.2
Si	14	26.04
Al	13	7.4

Fig. 7 (a) shows the SEM micrograph of surface modified of E-Glass fibre after immersing it into SBF for 14 days. A layer of apatite crystal growth could be observed over the fibre surface which was further confirmed by EDAX analysis [Fig. 7 (b)] of the fibre surface. E-glass fibre provided a biocompatible and bio-inert surface to SBF solution that promoted apatite layer deposition on its surface. The deposition of apatite layer on the surface of E-glass fibre acted as seed crystals for HA growth and entanglement around fibre surface on due course of hydrolysis of  $\alpha$ -TCP in SBF. Thus during setting reaction of CPC, a stronger interface between glass fibres and CPC crystals was formed. SBF treated E – glass fibres were mixed to the extent of 10 wt% with Si- $\alpha$  TCP powder, kneaded, formulated like a paste, hardened in SBF and mechanical strength of the resulted CPC was evaluated.

#### F. Analysis of Mechanical Strength

Fig. 8 shows the variation of diametral tensile strength with increase in soaking time in SBF for un-doped CPC, 1% Si doped CPC, and 10 weight% E-Glass fibres added Si doped CPC. In all the cases it was found that with increase in soaking time in SBF, DTS for CPC increased due to more amount of HA crystal growth and as a result of entanglement of HA crystals with each other to reduce porosity and enhance compactness in the microstructure. Higher degree of HA crystal growth and more entanglement of crystals in the pores of the microstructure of CPC gave better compactness with increase in elapsed time in SBF. As evident from the microstructure higher amount of macro porosity and lower

amount of compactness of un-doped CPC resulted in lower DTS as compared to Si doped CPC. The highest value of DTS was observed for E- glass fibre reinforced CPC which confirms the fact that addition of 10 wt % fibres in CPC matrix played vital role in enhancing the tensile strength of CPC.

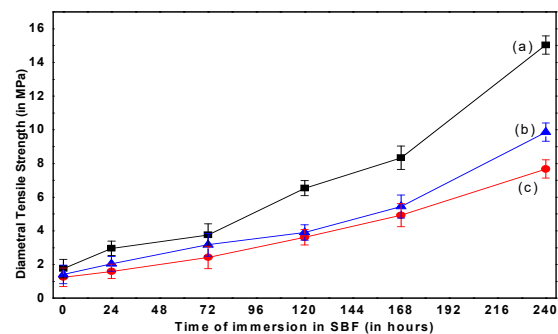


Fig. 8 Comparison of DTS of CPC with variation in soaking time in SBF (a) 1% Si doped  $\alpha$ -TCP with 10 weight% e-glass fibre, (b) 1% Si doped  $\alpha$ -TCP. (c)  $\alpha$ -TCP

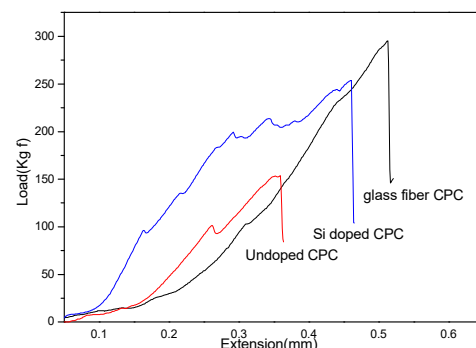


Fig. 9 Load vs extension graph of un-doped, Si doped and 10 wt% E –glass fibre reinforced Si doped CPC

Fig. 9 shows the load vs extension graph of un-doped and Si doped CPC reinforced with E glass fibre. It is evident that E-

glass fibre reinforced CPC failed at higher strain subsequently registering the highest tensile strength value among the CPC formulations. Thus ductility of the CPC samples increased in the order of un-doped CPC followed by Si doped CPC and

then fibre reinforced CPC. The higher tensile strength and ductility of Si doped CPC samples as compared to un-doped one may be attributed to lower porosity and greater compactness of the former.

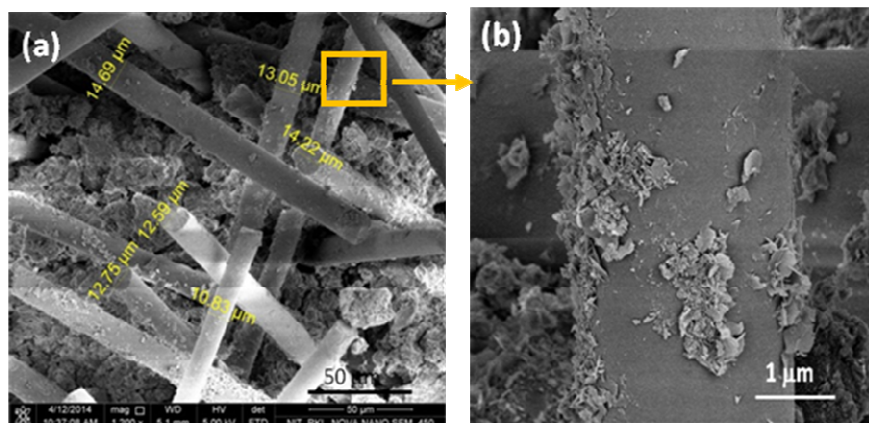


Fig. 10 (a) Fracture surface of 10 wt% E- glass fibre reinforced 1 mol% Si doped CPC (b) magnified image of fibre

Fig. 10 shows the fracture surface of fibre reinforced Si-doped CPC. It can be observed that addition of 10 weight% of E-glass fibre to Si-doped CPC filled up the voids in the microstructure as well as caused crack deflection to enhance strength in the composite structure. In addition, as evident from Fig. 10 (b) that the surface of E-glass fibre was coated with HA crystals that provided stronger interface between glass fibre and CPC grains.

#### G. MTT Assay

The effect of E glass fibre addition into CPC matrix on biocompatibility of CPC was assessed using MTT assay. MTT assay measures the cell proliferation ability of cultured cells on the surface of sample. As evident from Fig. 11 that keeping up with the positive control cultured MSCs on both Si doped CPC and fibre reinforced CPC proliferated up to 11 days. The number of viable MSCs on both Si doped and fibre reinforced CPC were not significantly different ( $p > 0.05$  for all period). This supports the fact that E- glass fibre addition into CPC matrix provides no significant effect in altering the biocompatibility of CPC.

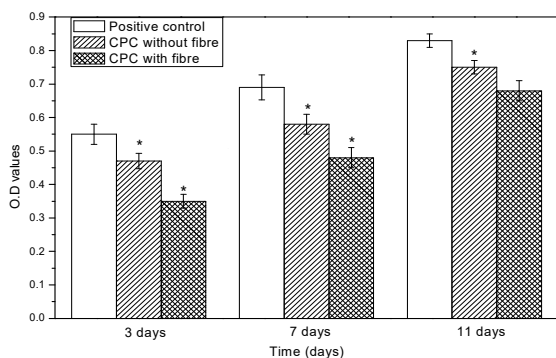


Fig. 11 MTT assay of CPC samples after culturing MSCs on its surface

#### VI. CONCLUSIONS

The objective of the present research was to enhance the mechanical strength of Si-doped CPC without compromising on its enhanced bioactivity. Effect of Si doping on the properties of  $\alpha$ -TCP based calcium phosphate cement was investigated. Doping with Si up to 1 mol% delayed the initial and final setting time of CPC. Si doped CPC exhibited a little slower rate of conversion into HA phase than that of un-doped CPC. One mol% Si doped CPC showed higher average diametral tensile strength than un-doped CPC at all-time points in SBF. Addition of 10 weight percent e-glass fibre onto 1mol% Si doped  $\alpha$  TCP resulted in almost 1.7 times increase in average diametral tensile strength of CPC. MTT assay of cultured mesenchymal stem cells on CPC samples proved that E-glass fibre addition into CPC had little effect on changing its biocompatibility.

#### ACKNOWLEDGMENT

The authors acknowledge the department of Ceramic Engineering at NIT- Rourkela for providing the necessary supports to carry out above research work.

#### REFERENCES

- [1] Dorozhkin, S.V., 2008. "Calcium orthophosphate cements for biomedical application". *Journal of Materials Science* 43, 3028–3057.
- [2] Larsson, S., 2010. "Calcium phosphates: what is the evidence?", *Journal of Orthopaedic Trauma* 24, 41–45.
- [3] Morgan, E.F., Yetkinler, D.N., Constantz, B.R., Dauskardt, R.H., 1997. "Mechanical properties of carbonated apatite bone mineral substitute: strength, fracture and fatigue behavior", *J. Mater. Sci., Mater. Med.* 8, 559–570.
- [4] Ginebra, M.P., Espanol, M., Montufar, E.B., Perez, R.A., Mestres, G., 2010. "New processing approaches in calcium phosphate cements and their applications in regenerative medicine", *Acta Biomater.* 6, 2863–2873.
- [5] Ginebra, M.P., Rilliard, A., Fernandez, E., Elvira, C., San Roman, J., Planell, J.A., 2001. "Mechanical and rheological improvement of a calcium phosphate cement by the addition of a polymeric drug", *J. Biomed. Mater. Res.* 57, 113–118.

- [6] Ishikawa, K., 2008. "Calcium phosphate cement", In: Kokubo, T. (Ed.), *Bioceramics and Their Clinical Applications*. CRC Press, Woodhead Publishing Ltd., pp. 438–463.
- [7] Lewis, G., 2006. "Injectable bone cements for use in vertebroplasty and kyphoplasty: State of the Art Review", *J. Biomed. Mater. Res. B* 76, 456–468.
- [8] Espanol, M., Perez, R.A., Montufar, E.B., Marichal, C., Sacco, A. Ginebra, M.P., 2009. "Intrinsic porosity of calcium phosphate cements and its significance for drug delivery and tissue engineering applications", *Acta Biomater.* 5, 2752–2762.
- [9] Martin, R.I., Brown, P.W., 1995. "Mechanical properties of hydroxyapatite formed at physiological temperature", *J. Mater. Sci., Mater. Med.* 6, 138–143.
- [10] Currey, J.D., Butler, G., 1975. "The mechanical properties of bone tissue in children", *J. Bone Joint Surg. A* 57, 810–814.
- [11] Morgan, E.F., Yetkinler, D.N., Constantz, B.R., Dauskardt, R.H., 1997. "Mechanical properties of carbonated apatite bone mineral substitute: strength, fracture and fatigue behavior", *J. Mater. Sci., Mater. Med.* 8, 559–570.
- [12] Nalla, R.K., Kinney, J.H., Ritchie, R.O., 2003. "Mechanistic fracture criteria for the failure of human cortical bone", *Nat. Mater.* 2, 164–168.
- [13] Callister Jr W.D., Rethwisch D.G. "Materials science and engineering: an introduction", 7<sup>th</sup> ed, John Wiley Sons Inc; 2009.
- [14] Hannant D.J., Hughes D.C., Kelly A. "Toughening of cement and other brittle solids with fibres", *Philosophical Transaction A* 1983; 310: 175–190.
- [15] Xu, H.H.K., Quinn, J.B., 2002. "Calcium phosphate cement containing resorbable fibres for short-term reinforcement and macroporosity", *Biomaterials* 23, 193–202.
- [16] Xu, H.H.K., Quinn, J.B., Takagi, S., Chow, L.C., Eichmiller, F.C., 2001. "Strong and macroporous calcium phosphate cement: effects of porosity and fibre reinforcement", *J. Biomed. Mater. Res.* 57A, 457–466.
- [17] Xu, H.H.K., Carey, L.E., Burguera, E.F., 2007a. "Strong, macroporous, and in situ-setting calcium phosphate cement layered structures", *Biomaterials* 28, 3786–3796.
- [18] Zuo, Y., Yang, F., Wolke, J.G.C., Li, Y., Jansen, J.A., 2010. "Incorporation of biodegradable electrospun fibres into calcium phosphate cement for bone regeneration", *Acta Biomater.* 6, 1238–1247.
- [19] Kean-Khoon Chew, Kah-Ling Low, Sharif Hussein Sharif Zein, David S. McPhail, Lutz-Christian Gerhardt, Judith A. Roether, Aldo R. Boccaccini, "Reinforcement of calcium phosphate cement with multi-walled carbon nanotubes and bovine serum albumin for injectable bone substitute applications", *Journal of the Mechanical Behavior of Biomedical Materials*, Volume 4, Issue 3, April 2011, Pages 331–339
- [20] Dos Santos, L.A., de Oliveira, L.C., da Silva Rigo, E.C., Garcia Carrodéguas, R., Ortega Boschi, A., Fonseca de Arruda, A.C., 2000. "Fibre reinforced calcium phosphate cement", *Artif. Organs* 24 (3), 212–216.
- [21] Xu, H.H.K., Eichmiller, F.C., Giuseppetti, A.A., 2000. "Reinforcement of a self-setting calcium phosphate cement with different fibres", *J. Biomed. Mater. Res.* 52, 107–114.
- [22] T. Kokubo, H. Kushitani, S. Sakka, T. Kitsugi and T. Yamamuro, "Solutions able to reproduce in vivo surface-structure changes in bioactive glass-ceramic A-W", *J. Biomed. Mater. Res.*, 24, 721-734 (1990).
- [23] Ginebra, M.P., E. Fernández, E.A.P. De Maeyer R.M.H. Verbeeck, M.G. Boltong, J. Ginebra, F.C.M. Driessens and J.A. Planell, "Setting reaction and hardening of an apatitic calcium phosphate cement", *J. Dent. Res.*, 76 905-912 (1997).